WILEY InterScience® DISCOVER SOMETHING GREAT

PROTEINS STRUCTURE ■ FUNCTION ■ BIOINFORMATICS

Monte Carlo folding of trans-membrane helical peptides in an implicit generalized Born membrane

Jakob P. Ulmschneider,[1]* Martin B. Ulmschneider,[2] and Alfredo Di Nola[1]

[1] Department of Chemistry, University of Rome "La Sapienza", Rome, Italy

[2] Department of Biochemistry, University of Oxford, Oxford, United Kingdom

ABSTRACT

An efficient Monte Carlo (MC) algorithm using concerted backbone rotations is combined with a recently developed implicit membrane model to simulate the folding of the hydrophobic transmembrane domain M2TM of the M2 protein from influenza A virus and Sarcolipin at atomic resolution. The implicit membrane environment is based on generalized Born theory and has been calibrated against experimental data. The MC sampling has previously been used to fold several small polypeptides and been shown to be equivalent to molecular dynamics (MD). In combination with a replica exchange algorithm, M2TM is found to form continuous membrane spanning helical conformations for low temperature replicas. Sarcolipin is only partially helical, in agreement with the experimental NMR structures in lipid bilayers and detergent micelles. Higher temperature replicas exhibit a rapidly decreasing helicity, in agreement with expected thermodynamic behavior. To exclude the possibility of an erroneous helical bias in the simulations, the model is tested by sampling a synthetic Alanine-rich polypeptide of known helicity. The results demonstrate there is no overstabilization of helical conformations, indicating that the implicit model captures the essential components of the native membrane environment for M2TM and Sarcolipin.

Proteins 2007; 69:297–308.

Key words: peptide folding; Monte Carlo; generalized Born; implicit membrane.

INTRODUCTION

Computational prediction of membrane protein structure remains one of the great challenges of theoretical biophysics. Interactions with the lipid bilayer environment are crucial for determining the correct fold. The two-stage model for α-helical proteins assumes that individual helices form across the membrane in a first step and subsequently assemble to form a functional protein.[1,2] This allows a stepwise approach.

Unfortunately, the complexity and large size of the cell membrane environment usually limits the use of realistic atomic detail lipid bilayer representations to very short timescales (ns), making membrane folding studies computationally unfeasible.[3,4] While it has been demonstrated that the folding of individual helices can in principle be simulated in explicit lipid bilayer membranes, the large computational resources required renders this approach unpractical to all but the most simple systems.[5] This has spurred the development of implicit solvent approaches, which enable significant gains in computational efficiency.[6,7]

The success of the generalized Born[8] method in globular protein and peptide folding simulations (see e.g. Refs. 9–13) has let to attempts to extend it to represent the membrane environment implicitly.[7,14–22] These models describe the membrane as a hydrophobic zone and have been used successfully to fold and assemble small helical membrane peptides.[16,17] Parameterization issues are largely avoided by being able to build on the large experience gathered with classical force fields, while introducing only a small number of new parameters. However, the detail of protein–solvent interactions, particularly hydrogen bonds is lost. This means care has to take to avoid simulation artifacts such as overstabilized salt bridges.[23]

Statistical analyses of membrane proteins[6] as well as translocon mediated insertion experiments of designed polypeptides[24,25] suggest that the insertion energy of a residue at a certain position along the membrane normal is a property of its local solvation environment. It therefore seems reasonable to model a membrane as a smoothly varying solvation function along the bilayer normal. Therefore, in the present study, the membrane was modeled as a region that becomes increasingly apolar (i.e. increasingly inaccessible to the solvent) towards its center using the generalized Born theory of solvation. The self-solvation energy of an atom, which accounts for the largest part of the solvation

Grant sponsors: Deutsche Forschungs-gemeinschaft (Emmy Noether fellowship), Wellcome Trust; Grant sponsor: MIUR FIRB Project; Grant number: RBIN04PWNC.
*Correspondence to: Jakob P. Ulmschneider, Department of Chemistry, University of Rome "La Sapienza", Rome, Italy. E-mail: Jakob@ulmschneider.com
Received 12 December 2006; Revised 5 February 2007; Accepted 12 February 2007
Published online 28 June 2007 in Wiley InterScience (www.interscience.wiley.com). DOI: 10.1002/prot.21519

energy,[26] was modified to vary smoothly between full solvation in bulk water and a limiting value for burial at the center of the membrane. At this stage of the development of the method any increased polarity at the charged bilayer interfaces was neglected. Nevertheless, the solvent exclusion properties of the membrane model account for the bulk properties of a lipid-bilayer. A general problem of membrane protein simulation lies in the correct treatment of charged residues at the membrane interfaces. In nature burial of a charged residue inside a membrane will almost certainly involve a change of protonation state or accompaniment by a hydration shell. Here the charged interfaces might play an important role, however, this is beyond the means of the present membrane model.

How well do current models and force-fields predict the correct conformational equilibria of polypeptide systems? Recently, there has been an increasing interest in attempts to explore if systematic biases in the parameter sets exist that influence secondary structure content.[27] Of crucial importance is the strength of backbone hydrogen bonds and backbone torsion potentials that play a dominating role in deciding the most favorable secondary structure of a sequence. If the backbone hydrogen bond is modeled too weakly, simulations from the experimentally determined native state will unfold even at physiological temperatures. If modeled too strongly, excessive formation of often erroneous secondary structure—usually helices—is observed, and energetic traps caused by strong inter-strand backbone contacts are formed. Experimental results indicate that the strength of the hydrogen bond depends strongly on the environment.[28] It is therefore difficult to calibrate implicit models by directly comparing the strength of specific interactions, but rather to observe the effect of those interactions on the conformational equilibria and the secondary structure content, which are more readily compared to experiment.

This issue is of fundamental importance to the modeling of membrane proteins, which have a large number of transmembrane helical motifs. If the model has a helical bias and the test system is a helix this problem will not easily be detected since folding will appear to proceed "correctly" in the simulations. To detect whether the simulation model is defective in this way, we use two strategies: First, a simple model system with experimentally known helical content is run for a very long time, and the determined helicity directly compared to experiment. Second, erroneous stability of helices is revealed by having a significant population of helical secondary structure even at elevated temperatures, where random coil conformations should prevail.

SIMULATION METHODS

The generalized Born membrane

The development of the present generalized Born (GB) membrane has been described in detail in a previous publication.[7] In particular, the Generalized Born equation[8] is left unchanged and only the method to calculate the Born radii is modified. The membrane is treated as a planar hydrophobic region in a uniform polar solvent with a dielectric constant $\varepsilon_w = 80$, that becomes increasingly inaccessible to the solvent towards its centre. Both the protein interior and the membrane are assumed to have the same interior dielectric constant of $\varepsilon_m = 2$. The Born radii are calculated using the fast asymptotic pair-wise summation of Qiu *et al.*[29]

$$G'_{\mathrm{pol},i} = \Gamma(z_i, R_i, L) + \underbrace{\sum_j^{1-2} \frac{P_2 V_j(z_j)}{r_{ij}^4} + \sum_j^{1-3} \frac{P_3 V_j(z_j)}{r_{ij}^4} + \sum_j^{1\leq 4} \frac{P_4 V_j(z_j)\ \mathrm{ccf}}{r_{ij}^4}}_{\text{sums only involving atoms with } |z| > L}, \quad (1)$$

where L is the membrane half width, z_i the z-position of the atom i, P_1-P_4 are the parameters determined by Qiu *et al.*,[29] the sums are over 1–2, 1–3, and $1 \geq 4$ neighbors and ccf is a close contact function. This method has been demonstrated to yield excellent results in predicting experimental free energies of solvation as well as hydration effects on conformational equilibria.[30] By modifying the pair-wise summation to solute atoms, the self-solvation terms $\Gamma(z_i, L)$ as well as the atomic volumes $V(z_i)$ were made to vary smoothly between full solvation and a limiting value for burial at the centre of the membrane. We propose a Gaussian shape

$$\Gamma(z_i) = g_{\mathrm{bulk}} + (g_{\mathrm{center}} - g_{\mathrm{bulk}}) e^{\gamma(z_i^2/L^2)}, \quad (2)$$

where g_{bulk} is the limiting value of Γ at a large distance from the membrane (i.e. $z \gg L$) corresponding to the self-solvation term of the unmodified generalized Born method $g_{\mathrm{bulk}} = -166/(R_i + \mathrm{offset} + P_1)$, while g_{center} is the value of Γ at the membrane center. We used a Gaussian with $\gamma = -3.0$ and membrane half width of $L = 15$ Å, while $g_{\mathrm{center}} = -7.67$ kcal/mol, as reported previously.[7,15,31]

The nonpolar part of the solvation free energy is modeled using an effective surface tension associated with the solvent accessible surface area (SA).[29] Instead of a costly calculation of the accurate SA, a mimic based on the Born radii is used, which has been shown to be very accurate, but much faster.[32] As it is moved towards the center of the membrane the surface energy contribution of each atom is scaled down by a Gaussian function of the same width as Γ. Thus for distances far from the membrane (i.e. $z \gg L$) the nonpolar contribution is included with the positive surface tension of solvation in water, while in the centre of the membrane the surface tension is negative, (i.e. energy is gained by moving into this phase from the gas phase) as determined experimentally.[33] The surface tension contribution of each atom was varied using a

 DOI 10.1002/prot

Gaussian function with $\gamma = -1.5$, interpolating between the limiting values of 12 cal/mol·Å^2 in bulk solvent and -19 cal/mol·Å^2 at the membrane centre.

It should be noted that the present membrane model neglects any effects due differences in lipid composition and charge distribution of the two bilayer leaflets as well as effects due to the trans-membrane voltage. However, it is in principle possible to include these properties by replacing the Gaussians with an equivalent nonsymmetric function.

The nonpolar part of the implicit membrane model was previously parameterized against experimental transfer free energies of hydrophobic side chain analogs,[33] and no parameters were optimized for the present simulations.

Monte Carlo sampling

The simulations were run with an all-atom Monte Carlo program developed by the authors specifically for the simulation of proteins in a GB/SA continuum solvent. An efficient concerted rotation sampling technique[34] is used to move the protein backbone; in addition there are single rapid side-chain moves, with a ratio of three side-chain moves per backbone move. The potential energy was evaluated with the OPLS-AA force field,[35] and the Monte Carlo simulations used Metropolis sampling. For M2TM and Sarcolipin, all nonbonded interactions as well as the GB energy were truncated using a cutoff of 14 Å, while no cutoffs were used for the smaller $(AAQAA)_3$ system. The Born radii were recomputed for every configuration. The described setup has been shown to perform well in sampling DNA[36] and protein folding simulations,[9] where the native state of several polypeptides was rapidly determined starting from extended conformations. We recently demonstrated that this method is equivalent to molecular dynamics sampling, with both methods able to find the native state of several polypeptides with comparable computational effort.[37]

The membrane spanning segment M2TM and Sarcolipin were modeled in completely extended conformation and simulated in an implicit membrane. The termini were acetylated and amidated respectively and the peptide was arranged so that it spans the membrane (Fig. 3). The principal experimental data for comparison with the present simulation results are structures of the M2TM segment obtained from solid-state NMR in lipid bilayers (PDB code 1MP6),[38] and solution NMR of Sarcolipin in detergent micelles (PDB code 1JDM),[39] as well as lipid bilayers.[40,41]

Replica exchange MC

The replica exchange method has recently been reviewed in detail.[42,43] Ten replicas of each system were set up with identical fully extended initial configuration and exponentially spaced temperatures in the range 300–500 K for M2TM and Sarcolipin and 274–500 K for $(AAQAA)_3$. Every 10^4 Monte Carlo moves a replica swap with transition probability

$$p_{1\rightarrow 2} = \exp(-\Delta), \tag{3}$$

where

$$\Delta = \left(\frac{1}{kT_1} - \frac{1}{kT_2}\right)(E_1 - E_2) \tag{4}$$

is attempted. E_1 and E_2 are the total energies of two conformers at temperatures T_1 and T_2, respectively. High temperature replicas facilitate the crossing of energy barriers, while low temperature replicas extensively sample low energy conformations. This enables the efficient and increased sampling of the entire system by frequent crossing of high energy barriers. The exponential temperature spacing ensures a constant acceptance rate of all adjacent replica swaps.[42]

Analysis

The free-energy was calculated as a function of the root-mean-square C_α deviation (RMSD) from the experimental structure (PDB code: 1MP6). For a system in thermodynamic equilibrium, the change in free energy on going from one state to another is given by

$$\Delta G = -RT \ln\frac{p_1}{p_2} \tag{5}$$

where R is the ideal gas constant, T is the temperature and p_i is the probability of finding the system in state i. The RMSD was divided into a grid with a spacing of 0.5 Å, and the free-energy was calculated for each bin. In addition, the average total system energy E was calculated for each cell, which is the sum of peptide internal energy plus the interactions with the solvent and membrane given by the GBSA solvation free energy. To check the effect of a different grid size on the thermodynamic properties, different grid spacings of 0.1–0.5 Å were used to construct the same free-energy landscapes. Surfaces constructed on smaller bin sizes tended to be rougher as fewer points are available per bin, but all are similar, with the same overall shape and spread of the free-energy.

RESULTS AND DISCUSSION

$(AAQAA)_3$

As a test system, we chose a 15 residue synthetic peptide with the sequence $(AAQAA)_3$, which has been used to evaluate helical propensity in a large family of alanine-rich peptides.[44] Experimentally, the system shows an average helicity of 44% at 274 K by NMR measurements.[45] The system was modeled in bulk solvent using the GBSA

implementation of Qiu *et al.*[29] as described for previous folding simulations.[9,37] A replica exchange MC (REMC) run was performed using 10 replicas from 274–500 K and 10 billion MC step length per replica. This setup was chosen since REMC simulations performed using only five replicas—as well as individual trajectories at 274 K—did not generate sufficiently converged results. The beginning of the chain was acetylated and the chain end amidated, as in the experiments. All replicas started from completely extended conformations. A residue is considered helical if it belongs to a segment of at least two residues whose backbone dihedral angles (ϕ, ψ) are within 40° from the ideal α-helical values ($-57°$, $-47°$). During the simulations, the system revealed extensive sampling of coiled as well as helical and β-hairpin structures, with no clearly defined stable conformation. The overall helicity of the peptide over the course of the simulation is shown in Figure 1 for 274 K and 500 K. At 274 K there are significant fluctuations in helical content, whereas almost none are observed at 500 K. The helicity of each residue was averaged over the entire simulation and for each temperature replica. Figure 2 shows the results for the lowest replica at the experimental temperature of 274 K. Because of many folded and unfolded conformations at this temperature, the average helicity per residue has a standard deviation of about $\pm$20% (error bars in Fig. 2). As in the experiments, the helicity is lower at the chain ends, which were frayed and flexible throughout the simulations. The overall helicity is only 17%, less than half of the experimental average helicity of 44%. There are various definitions of "helicity" in use, so a perfect match to the experimental work is not expected. The inset of Figure 1 shows the temperature dependence of the overall helicity, revealing the steady decline from the experimental 274 to 500 K.

To investigate the role of the solute interior dielectric constant, which was $\varepsilon = 1$ here, but has a value of $\varepsilon = 2$ in the implicit membrane model, the simulations of $(AAQAA)_3$ were repeated with $\varepsilon = 2$. The helicity was almost identical (data not shown). The only difference was the slightly reduced dynamics, since the Coulombic interactions are less well compensated by the GB energy, resulting in a higher frequency of trapped conformations during the simulations. Thus, the helicity of the system is not very sensitive to the chosen value of ε.

There are several previous simulation studies of this system with relatively short sampling time of 1–10 ns, using sigmoidal dielectrics (10 ns),[48] explicit water ($\sim$1 ns),[49] mean solvation models (2 ns),[50] and self-guided MD (10 ns).[51] All report an average helicity close to experiment—although the simulations are likely not converged. Good agreement is also reported by recent Monte Carlo studies using a conformational memory MC approach with an implicit screened Coulomb model,[52] and a MC study where the peptide is modeled as series of beads.[53]

However, these results are contrasted by the more detailed MD simulations on much longer timescale (4 μs) performed by Ferrara *et al.*,[46] where the peptide was found almost entirely helical, with an overall helicity of 75%, and the center residues showing a helicity of $\sim$90% (Fig. 2). A 30-ns run starting from a completely α-helical structure was shown to remain folded, with a C_α-RMSD mainly below 2 Å throughout the entire simulation [Fig 3(a) of Ref. 46]. Recently, the problem of erroneous high helicity has been summarized excellently by Chen *et al.*[47] and Im *et al.*,[18] who also found a much higher helicity of this system using a generalized Born implicit solvation model. An overall helicity of $>$85% is reported [Figs. 3(b) and 5(a) of Ref. 18] at 274 K. The authors propose a correction of atomic GB radii to compensate for the erroneous helix stability, which yields much improved helicities, closer to the experimental results (Fig. 2).

In our study of $(AAQAA)_3$, using the OPLS-AA force field,[35] and the Generalized Born model based on the parameterization of Qiu *et al.*,[29] no overstabilization of helical structures was found, in fact the helicity is underestimated compared to experiment. The results could be brought to a closer match using a similar procedure as suggested by Im *et al.*[18] by slightly tuning the radius of the amide nitrogen. But the success of the implicit membrane model in obtaining correctly folded helical structures (see below) indicates such an optimization is not necessary for studying TM helices. More importantly, there is clearly no helical bias in the model. For the subsequent simulations of helical membrane peptides in this work, an intrinsic tendency of our model to generate helices—no matter what the input sequence—can therefore be ruled out.

Influenza A

The M2 protein from *influenza A* virus is a 97-amino-acid protein with a single transmembrane helix that forms proton-selective channels vital to the function of the virus. In this work, we study the folding of the hydrophobic transmembrane domain M2TM (residues 22–46 of M2), a 25-residue α-helical motif that is essential to the formation of functional tetramers in membrane environments. M2TM has been investigated using a variety of experimental methods,[54–58] and solid-state nuclear magnetic resonance spectroscopy (NMR) measurements reveal that M2TM is a stable membrane spanning α-helix in bilayers.[38,59,60] In the present work we concentrate on the first step of the two-stage pathway, the folding of a trans-membrane helical monomer.

Previous simulation work on this system has chiefly concentrated on modeling of the channel arrangement in membrane environments.[61–65] Folding of M2TM has recently been studied by Im and coworkers using a similar GB-based implicit membrane model.[16] In the present study REMC simulations were run with 10 replicas for 2.2 $\times$ 10^9 MC steps each (see *Methods*), starting from completely extended conformations perpendicular to the

 DOI 10.1002/prot

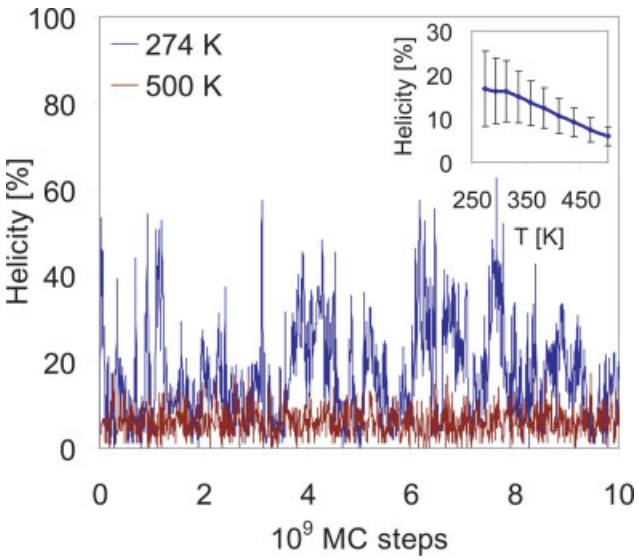

Figure 1

Overall helicity of $(AAQAA)_3$ over the course of the simulation at 274 K (first replica) and 500 K (last replica). There are frequent transitions of helical, partly-helical and coiled conformations at 274 K. At 500 K, the system shows almost no helical content. Inset: *Overall helicity of $(AAQAA)_3$ as a function of the replica temperature.*

membrane plane. Figure 3 shows the folding progress of the trans-membrane system over the course of the simulation. Only three of the 10 replicas are displayed for clarity. The lowest three temperature replicas (300–336 K) fold into continuous trans-membrane helices. Replicas with a temperature higher than 356 K (i.e. 356–500 K) retain a large amount of extended conformations and do not form stable membrane spanning helices. Nevertheless they contain a large amount of helical secondary structure. Particularly at the interfacial regions partial helices form frequently, while the centre of the trans-membrane spanning segment is generally unfolded. Some of these coiled and partly helical structures have moved completely outside of the membrane in several higher temperature replicas.

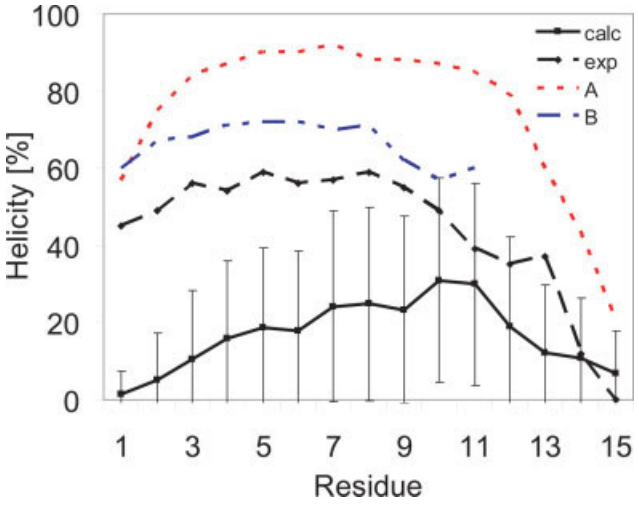

Figure 2

Simulated and experimental residue helicity of $(AAQAA)_3$ at 274 K. The helical content was averaged over the whole simulation. A residue is considered helical if it belongs to a segment of at least two residues whose backbone dihedral angles (ϕ, ψ) are within 40° from the ideal values (−57°, −47°). Experimental results from Shalongo et al.[45] *Also shown are the simulation results from Ferarra et al.*[46] (***A***) *and Chen et al.*[47] (***B***).

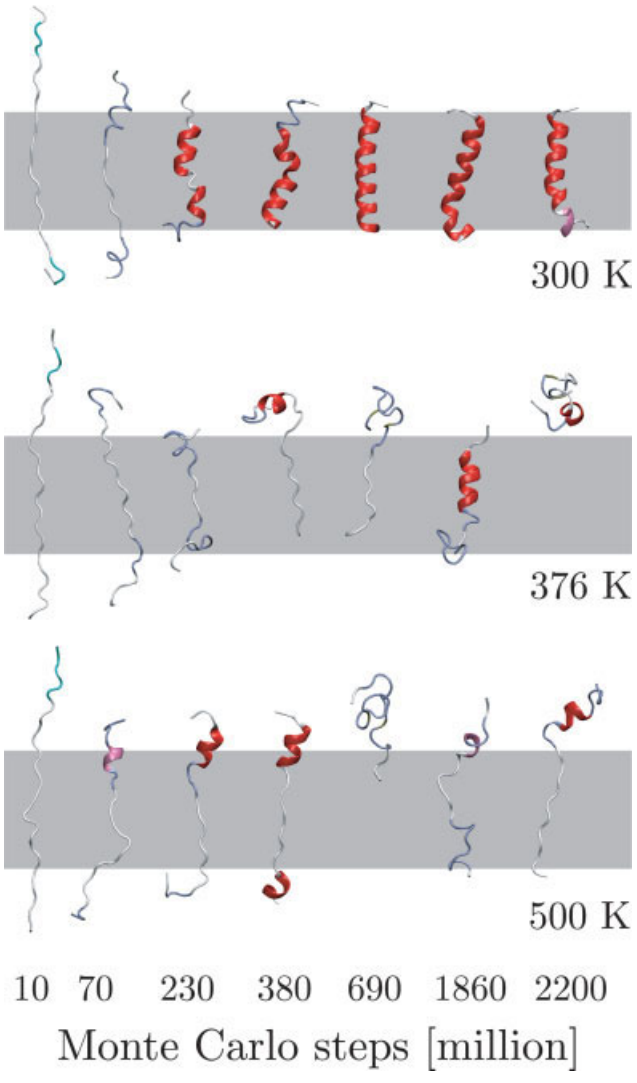

Figure 3

Trans-membrane folding of the M2TM monomer as a function of temperature. Only three replicas are shown for clarity. The lowest three temperature replicas (300, 318, and 336 K) fold into stable membrane spanning helices within the first ~300 million Monte Carlo steps, while the higher temperature replicas retain largely extended or coiled conformations. Some of the higher temperature replicas have exited the membrane. It should be noted that the implicit membrane does not represent a hydrophobic slab but rather a Gaussian shaped hydrophobic zone, thus the 30 Å slabs shown are for reference only.

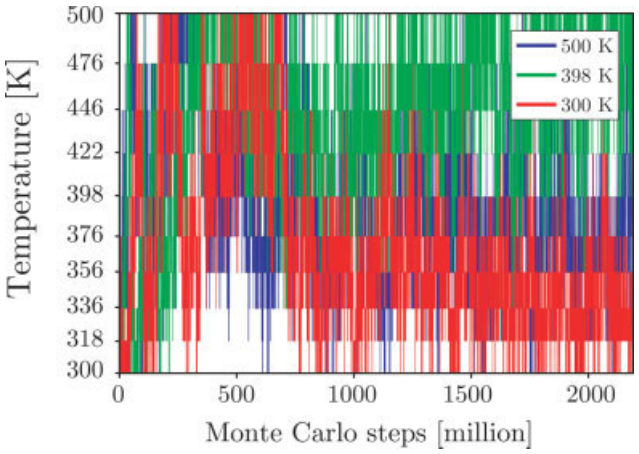

Figure 4

Temperature versus simulation time for the 300, 398, and 500 K starting simulations of the membrane system. The other replicas behave identically and have been omitted for clarity. [Color figure can be viewed in the online issue, which is available at www.interscience.wiley.com.]

There is virtually no beta structure except occasionally at the interfaces. Interestingly the helix formation of the lower replicas initiates at the interfaces as well. The ability of the interfacial regions to provide a strong catalyst for secondary structure formation is well known and generally attributed to its amphiphilic nature.[66]

The efficiency of the REMC algorithm can be seen in Figure 4, where the fluctuation of the temperature over the course of the simulation is shown. Each replica samples the whole temperature space of the simulations (only the 300, 398, and 500 K are shown for clarity, the others are exactly similar). Once a particular starting structure folds into a low free-energy conformation (e.g. a transmembrane helical conformation, 300 K line) it remains in the low temperature range of the replicas. Contrary a structure that retains an unfolded or extended conformation is heated, and remains in high temperature replicas until it forms low energy secondary structure, which in turn will initiate its temperature descend. This means that replicas that are "stuck" in a non-native conformation are slowly pushed up the temperature ladder and consequently melted since structures closer to the native state are being passed down.

We would like to point out that although it is possible to simulate membrane proteins in implicit membrane representations at the higher temperatures, the model is not physically correct since real membranes would disintegrate at such high temperatures. In the implicit model, the membrane always remains intact irrespective of the temperature. The REMC runs serve only to speed up sampling at the relevant low temperature of 300 K, and obtain the thermodynamic data at 300 K faster. Data for the higher temperatures will almost certainly not match experimental results.

To quantify the similarity to the native state, we aligned each conformation to the C_α positions of the experimental structure (Ser 22—Leu 46 of 1MP6) and calculated the RMSD. For three representative replicas spanning the entire temperature range, the results are shown in Figure 5 (lower panel). All folding events take part in the first ~300 million MC steps, with a rapid decline in RMSD until a steady state is reached. Low temperature replicas can be seen to have lower RMSD, being closer to the native state. The corresponding graph of the overall system helicity is shown in the upper panel of the same figure. Helical content is clearly strongly dependent on the temperature, with highest helicity for the 300 K replica. Since there are frequent replica swaps at constant temperature, both the RMSD and helicity fluctuate widely. It can be seen that the lowest replica mainly cycles between a fully

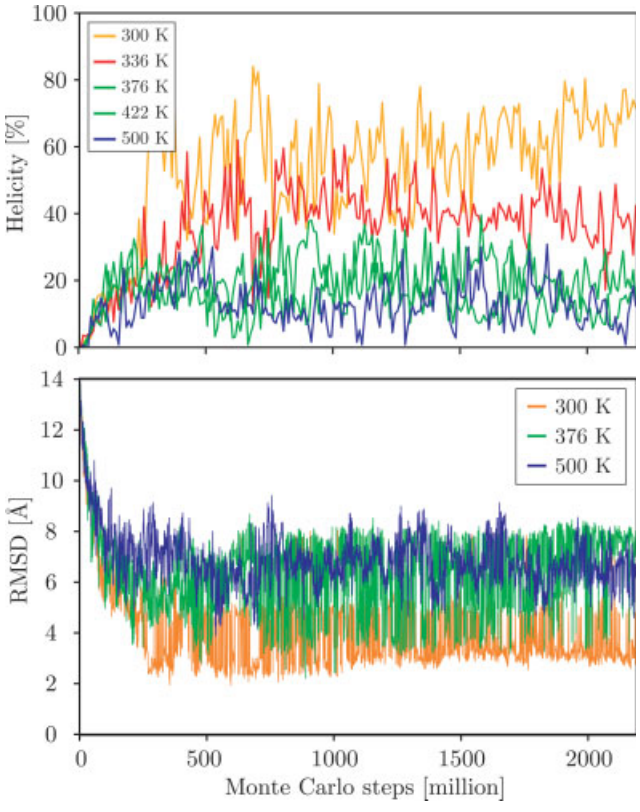

Figure 5

Lower panel: *Root mean square C_α-deviation from the NMR structure of M2TM (PDB code 1MP6) plotted against simulation time for the three replicas of 300, 376, and 500 K. Since replicas are swapped, the fluctuation is large. A clear correlation of RMSD with temperature is evident, with the lowest replica closest to the experimental structure.* Upper panel: *Average helicity of the system as function of simulation time for various replicas. [Color figure can be viewed in the online issue, which is available at www.interscience.wiley.com.]*

DOI 10.1002/prot

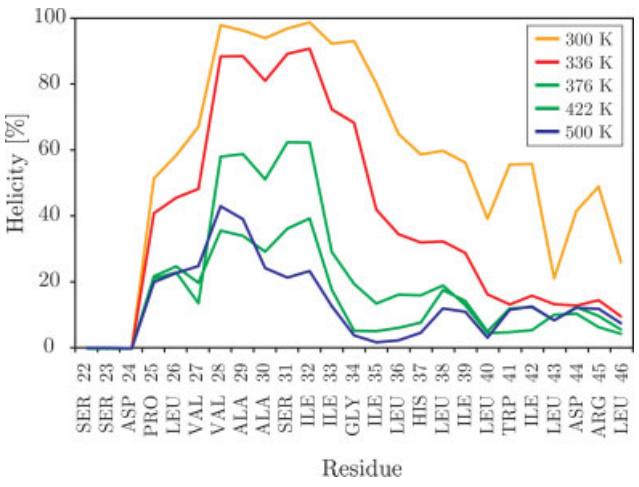

Figure 6

Average helicity versus residue for various replicas of the membrane folding run. The membrane system displays strong temperature dependence. The averages were over the last 1.9 billion Monte Carlo steps. [Color figure can be viewed in the online issue, which is available at www.interscience.wiley.com.]

folded helix (RMSD ~2.5 Å) and an almost fully folded helix, where residues 38–46 are partly unfolded (RMSD ~4 Å). The helicity graph has been smoothed by plotting the bin averages of every 10 consecutive conformations, and the same fluctuation is visible.

Of special interest is the distribution of the average helicity along the chain, shown in Figure 6 for each residue as a function of replica temperature. The equilibration time of the first 300 million MC steps is not included in the averages. Again the system displays a strong temperature dependence, with rapid decrease in helicity for rising temperature, most apparent at the core of the membrane spanning segment. The lower helicity of ~60% for residues Leu36-Leu46 is due to averaging a completely folded replica and an almost folded replica, as noted above for the RMSD plot. Also, the chain ends are found to be frayed and mostly do not sample helical conformations.

Structural stability of the trans-membrane configuration

Figure 7 shows the tilt angle and centre of mass (CM) movement along the membrane normal of the peptide over the course of the simulation, for the 300 and 500 K replicas. While lower temperature replicas remain firmly integrated into the membrane due to the strongly charged termini, some of the higher temperature replicas sample unfolded structures outside the membrane at up to 25 Å CM distance. There are occasional swaps of these structures into low temperature replicas as can bee seen by spikes in Figure 7, but they contribute little to the sampling at the low temperature since the simulation quickly reverts back to energetically much lower inserted TM conformations during the next swap move. At 300 K, the system displays small movements along the membrane normal, with the CM of the helices usually oscillating around a simulation average of $+0.6 \pm 3.3$ Å.

The helix shows a tendency to tilt frequently in the range 0–30°, (upper panel of Fig. 7) with only a slight influence of the system temperature, demonstrating that the system retains a large conformational flexibility even at low temperatures. The mean tilt angle of the 300 K replica was found to be $(12 \pm 7)^\circ$, which is at the lower end of the ~15–38° experimentally reported tilt angel range.[64] It has been argued that the tilt angle is dependent in a simple geometric way on the lipid bilayer thickness due to the preferred burial of the hydrophobic part of the helix in the bilayer ("hydrophobic mismatch").[64] Estimates of hydrophobic thickness for common lipids are DLPC, 19.5 Å; DMPC, 23.0 Å; DOPC, 27 Å; and POPC, 26.5 Å,[67] and recent experimental results seem to confirm this mechanism, which would explain the lower tilt angle for the membrane thickness of 30 Å in our model. However, solid

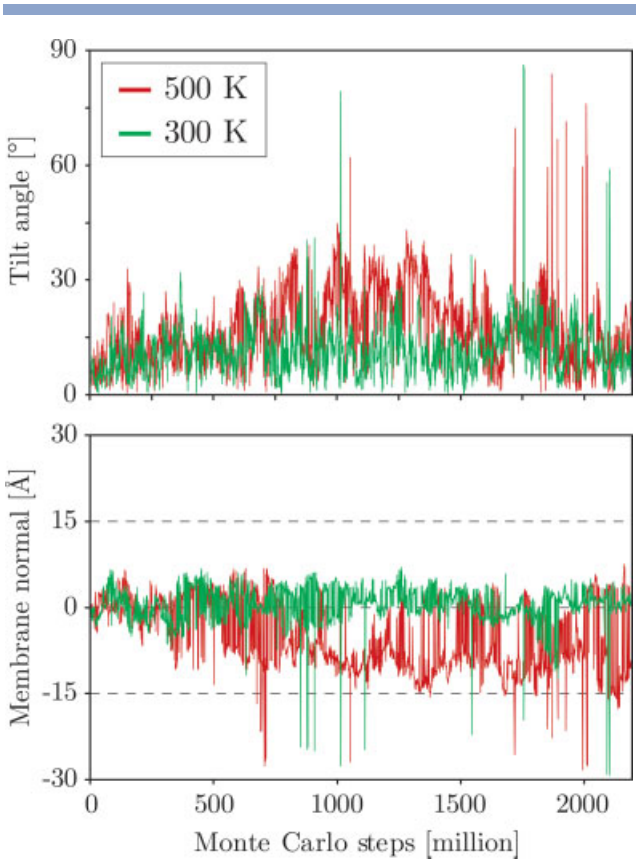

Figure 7

Tilt angle and centre of mass z-position versus simulation time for various temperature replicas of the membrane systems. [Color figure can be viewed in the online issue, which is available at www.interscience.wiley.com.]

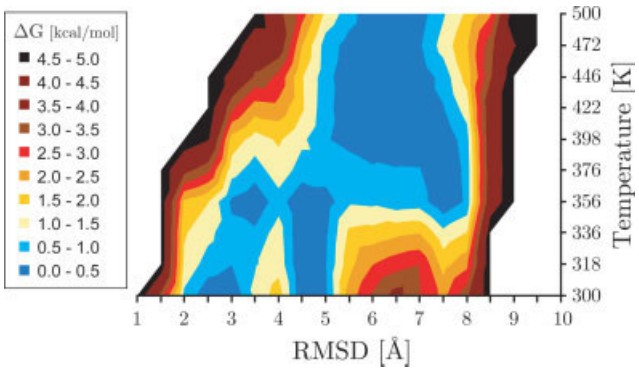

Figure 8

One dimensional free-energy (ΔG) as a function of RMSD from the native structure for each replica. The lowest states encountered were defined as the zero potentials. The free energy minimum shifts from helical conformations (RMSD = 2–3 Å) at low temperature to mis- and unfolded structures at high temperatures (RMSD >5 Å), with the transition temperature ∼350 K. [Color figure can be viewed in the online issue, which is available at www.interscience.wiley.com.]

state NMR studies on M2TM give a helix tilt of (37 ± 3)° in DMPC and a similar (33 ± 3)° in the thicker DOPC,[38,59,60] suggesting little influence of the lipid environment on tilt. The difference could also be due to the tetrameric form of M2TM in the NMR experiments,[38,60] resulting in a tilt being less sensitive on the membrane thickness than the monomers used in the simulations. We would like to note that the implicit membrane used in our model neglects any effect of the difference in lateral pressure of different lipids. Also, the lipid phase is ordered and nonisotropic, which should strongly determine helix tilting, yet this is not at this point implicitly included in the model. A dependence of the tilt angle on the membrane thickness was also found in the GB simulations of M2TM by Im *et al.*, who report 43° for a membrane thickness of 25 Å and 28° for a thickness of 29 Å.[16] In our model, the tilt angle could be easily increased by the tuning of γ that determines the strength of the Gaussian hydrophobic zone. However, any modifications of the implicit membrane must improve the results for all studied TM systems, and such further parameterization is currently under way involving a large set of membrane spanning peptides.

Free energy as function of similarity to the NMR structure

Low temperature replicas exhibit steady folding of the trans-membrane helices within the first 300 million MC steps. Higher temperature replicas stay further away from the native state and do not form stable TM helices. We calculated a series of one-dimensional free energy profiles as a function of the C_α-RMSD to the NMR structure. The results are shown in Figure 8, with the profiles for all temperatures in one graph. The reported values are in kcal/mol above the minimum encountered for each temperature—each temperature has its own bin with zero free energy (this is not a two-dimensional free energy map), and the first 300 million MC steps are omitted in the calculation. The change of the free energy profile as the temperature is increased is clearly visible: At $T = 300$ K, there are only helical structures, with the complete TM helix and the partly formed helix mentioned above populated. Replicas higher than a transition temperature of ∼350 K sample only non-native structures.

Our result differs from the GB REMD simulations of Im *et al.* who found all eight replicas ranging from 300–500 K to fold into helices.[16] The timescale of helix formation (∼13 ns) is also twice as fast as encountered in our

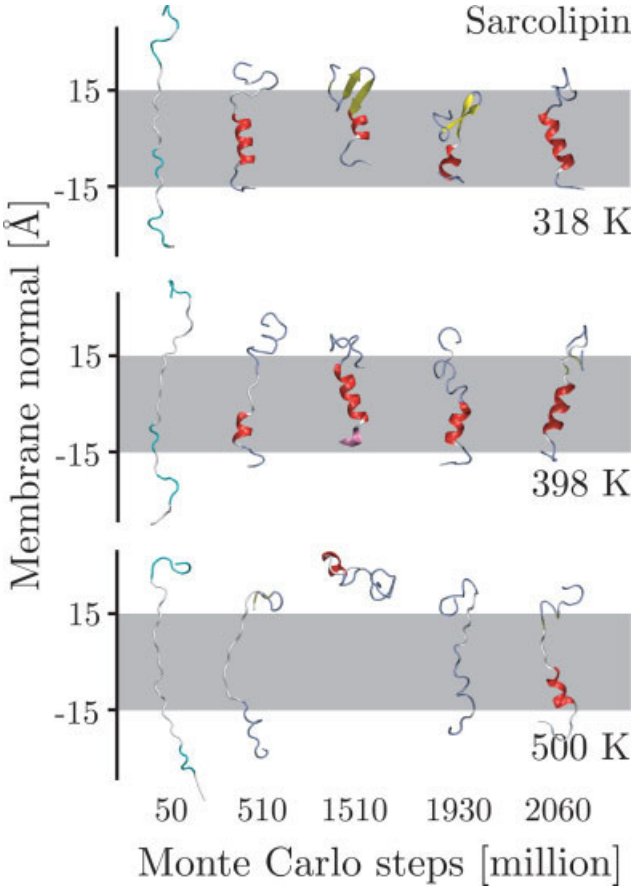

Figure 9

Folding of Sarcolipin as a function of temperature. Only three replicas are shown for clarity. The lower temperature replicas fold into stable conformations with a strong helical segment for the residues 14–27 within the first ∼300 million Monte Carlo steps, while the highest temperature replicas retain largely extended or coiled conformations. Occasionally, β-structures are observed - illustrated here for 318 K - but the helical conformations strongly dominate. [Color figure can be viewed in the online issue, which is available at www.interscience.wiley.com.]

DOI 10.1002/prot

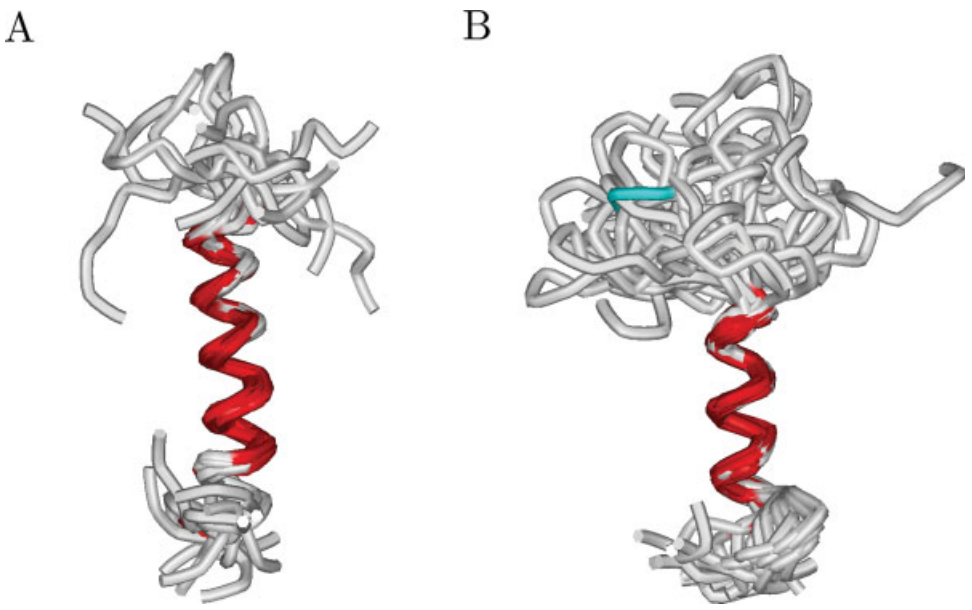

Figure 10

*(**A**) Overlay of the 16 conformers of Sarcolipin determined in the NMR measurements at 323 K (PDB code 1JDM). (**B**) Overlay of representative structures from the stable folded phase encountered in the simulations at 318 K. In both experiment and simulation, the N-terminal and C-terminal residues are unstructured. The helical segment is more stable by one helical turn in the experiments (Phe 9 to Ile 14) as compared to the simulations. [Color figure can be viewed in the online issue, which is available at www.interscience.wiley.com.]*

runs: 300×10^6 MC steps $= 13 \times 10^6$ MC scans ≈ 26 ns, where we assume 1 MC scan $\approx$1 MD time step.[37] The high stability of the helix even at 500 K could be due to a helical bias in the simulation model used, and the authors discuss this in detail in a recent analysis.[18] In the present study, the physically correct thermal behavior is seen, with a stable TM helix only at physiological temperature and random structures at high temperatures. A helical tendency of the OPLS parameters in combination with our GB model was shown to be unlikely above for the case of $(AAQAA)_3$. Thus the membrane environment and the specific sequence seem to be the sole contributors to form M2TM as a helix in our simulations.

In order to test the reproducibility of the folding results, a second REMC run was performed using a similar setup, only with a larger number of 25 replicas ranging from 300–700 K. Due to the larger number of replicas, the simulations were only run up to $\sim 700 \times 10^6$ MC steps. The results were found almost identical, with fully folded TM helices for the low temperature replicas after about $\sim 400 \times 10^6$ MC steps, demonstrating the correct folding behavior is not dependent on the details of the REMC setup.

Sarcolipin

Sarcolipin is an integral membrane protein that regulates the activity of the sarco(endo)plasmic reticulum calcium pump Ca^{2+}-ATPase (SERCA) in skeletal muscle.[68] A high-resolution structure of the 31 residue peptide (sequence MGINTRELFLNFTIVLITVILMWLLVRSYQY) in sodium dodecyl sulfate (SDS) micelles and its orientation in lipid bilayers is available by solution and solid-state NMR methods, respectively.[39] These measurements indicate that the system adopts a highly defined α-helical conformation from Phe 9 through Arg 27, while the N-terminus (residues 1–8) and the C-terminus (residues 28–31) are mostly unstructured. When buried in phospholipid bilayers, the experiments reveal a TM insertion perpendicular to the membrane plane, while other NMR studies indicate a tilt of $\sim 23^\circ$.[40]

REMC simulations were run in a similar fashion to the M2TM runs with 10 replicas for 2×10^9 MC steps each, starting from completely extended conformations perpendicular to the membrane plane. Figure 9 shows the folding progress over the course of the simulation. Quick formation of α-helical conformations in TM orientation is observed, while the highest temperature replicas sample mostly unfolded structures. In addition to helical conformations, some of the lower temperature replicas sample also β-structures inside in the membrane, as illustrated for 318 K—indicating a wide spread of conformations are sampled. However, the β-content is only populated for a very short time and does not contribute significantly to the conformational averages.

Similar to the experiments, Sarcolipin is found to form a TM helix for the center residues, while the other residues appear to be unstructured. In the simulations, the stable part of the helix ranges from Val 15 to Arg 27, involving 13 residues. While the match of the helical segment on the C-terminus is correct, one turn (from Phe 9 to Ile 14) on the N-terminal side is more stable in the experiment than in the simulation. This is visualized in Figure 10, by overlaying representative structures from the folded phase of the runs at 318 K and comparing to the overlay of the 16 NMR structures (at 323 K). Figure 11 shows the corresponding backbone RMSD to the experimental structure (conformer 7 of 1JDM) as well as the average helicity for each residue for the replica at 318 K. In the experiments, only residues 9–27 where used in the fitting. Similarly, for the simulations only the helical section involving residues 14–27 is fit. Other than the helical turn involving Phe 9—Ile 14, the match to the experiment is remarkable given the simplicity of the implicit GB membrane. In both experiment and simulation the C-terminus (residues 28–31) and N-terminus (residues 1–8) have no stable conformation, helical or otherwise.

The structural subdomains found in the simulation are similar to the ones found in solution NMR studies in dodecylphosphocholine (DPC) detergent micelles,[41] which revealed an unstructured N terminus (residues 1–6), a short dynamic helix (residues 7–14), a more rigid helix (residues 15–26), and an unstructured C terminus (residues 27–31). The rigid helix is perfectly reproduced in the simulations. The short dynamic helix (residues 7–14) exhibits faster motion in the experiments, probably due to the larger hydrophilicity of the residues. The low helicity found for this section in the simulations, involving Phe 9 and Phe 12, could also be due to the deficiency of the implicit membrane to accurately model nonpolar aromatic effects.

The native state of Sarcolipin is found much more stable at elevated temperatures than M2TM, with the helical segment formed even for higher temperature replicas. In comparison to the results for M2TM, full helices are not formed even at low temperature, in agreement with the experimental results. The system remains quite flexible in the membrane, with an average CM z-position of $+0.3 \pm 6.3$ Å. The helical domain shows a tendency to tilt frequently in the range $(0–40)^\circ$, with only a slight influence by the system temperature. The mean tilt angle of the 318 K replica was found to be $(16 \pm 8)^\circ$. This is close to the $\sim 23^\circ$ reported in DOPC/DOPE lipid bilayers.[40] Thus the overall agreement with experiment is excellent.

CONCLUSIONS

The present study demonstrates that an implicit generalized Born membrane in combination with all-atom force fields and an efficient Monte Carlo sampling scheme can reliably predict the native state of the membrane spanning M2TM peptide from *influenza A*, as well as of Sarcolipin. Use of a replica exchange algorithm yields reasonably converged thermodynamic properties and a free-energy surface at much shorter timescales than would be required otherwise. The total simulation effort involved an accumulated time of 4.2×10^{10} MC steps, corresponding roughly to ~ 2.7 μs of molecular dynamics.[37] The membrane simulation of M2TM folded full membrane spanning helices with the low temperature replicas sampling conformations to within 2.5 Å of the native state. The sarcolipin runs do not form continuous TM helices: the system segments into several domains with a stable helix, a dynamic helical turn and unstructured termini, very similar to the structures observed in the NMR experiments. Once the helices have formed in the low temperature replicas they remain stably integrated into the membrane. Nevertheless, they retain a large conformational flexibility

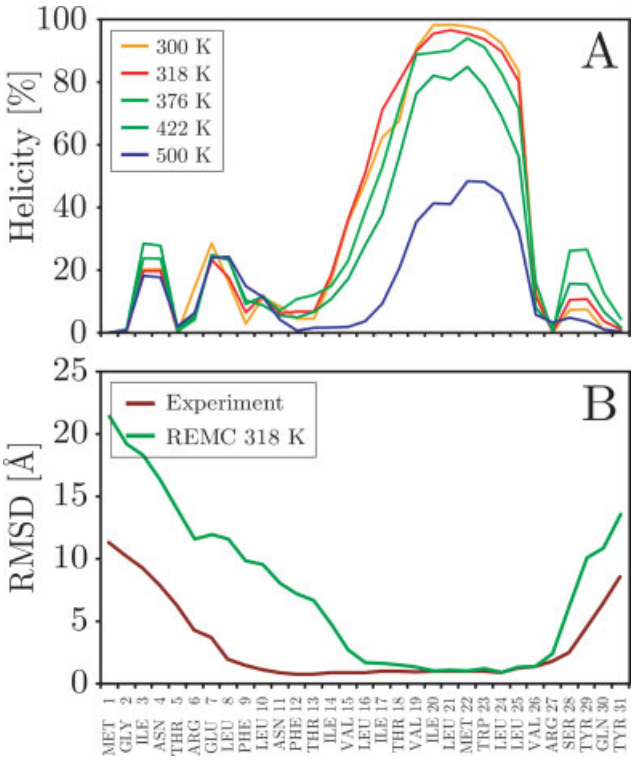

Figure 11

*(**A**) Average helicity per residue for several temperature replicas. The helical section is slightly smaller than in the experiment, and shows significant thermal stability. (**B**) Average backbone RMSD to the experimental structure (conformer 7 of 1JDM) per residue. The average is over the entire 318 K replica, with only the first 300 M steps of equilibration excluded. Structures were superimposed using residues 14–27 only. The red line gives the average backbone RMSD per residue as found in the NMR measurements, where residues 9–27 were used in the fitting.[39] [Color figure can be viewed in the online issue, which is available at www.interscience.wiley.com.]*

DOI 10.1002/prot

exploring the vicinity of the native state by frequent tilting, kinking and bending.

Higher temperature replicas remained unfolded. Together with a verification of the model using a synthetic Ala-rich peptide, which revealed there is no intrinsic helical bias in the simulation parameters, this result demonstrates that it is the membrane environment that is crucial to determining the correct fold of the protein. The different behavior of M2TM and Sarcolipin demonstrates that the model does not simply favour all-helical TM conformations but that the sequence crucially influences the structure. Further work is under way to investigate the role of the solute dielectric constant and the folding properties in bulk solvent as compared to the implicit membrane. We are currently exploring the application to larger systems and investigating the performance and accuracy compared to all-atom lipid bilayer membranes and coarse grain approaches.

REFERENCES

1. Engelman DM, Chen Y, Chin CN, Curran AR, Dixon AM, Dupuy AD, Lee AS, Lehnert U, Matthews EE, Reshetnyak YK, Senes A, Popot JL. Membrane protein folding: beyond the two stage model. FEBS Lett 2003;555:122–125.
2. Popot JL, Engelman DM. Membrane-protein folding and oligomerization—the 2-stage model. Biochemistry 1990;29:4031–4037.
3. Forrest LR, Sansom MSP. Membrane simulations: bigger and better? Curr Opin Struct Biol 2000;10:174–181.
4. Efremov RG, Nolde DE, Konshina AG, Syrtcev NP, Arseniev AS. Peptides and proteins in membranes: what can we learn via computer simulations? Curr Med Chem 2004;11:2421–2442.
5. Nymeyer H, Woolf TB, Garcia AE. Folding is not required for bilayer insertion: replica exchange simulations of an alpha-helical peptide with an explicit lipid bilayer. Proteins 2005;59:783–790.
6. Ulmschneider MB, Sansom MS, Di Nola A. Properties of integral membrane protein structures: derivation of an implicit membrane potential. Proteins 2005;59:252–265.
7. Ulmschneider MB, Ulmschneider JP, Sansom MSP, Di Nola A. A generalized Born implicit membrane representation compared to experimental insertion free energies. Biophy J 2007;92:2338–2349.
8. Still WC, Tempczyk A, Hawley RC, Hendrickson T. Semianalytical treatment of solvation for molecular mechanics and dynamics. J Am Chem Soc 1990;112:6127–6129.
9. Ulmschneider JP, Jorgensen WL. Polypeptide folding using Monte Carlo sampling, concerted rotation, and continuum solvation. J Am Chem Soc 2004;126:1849–1857.
10. Chowdhury S, Zhang W, Wu C, Xiong GM, Duan Y. Breaking nonnative hydrophobic clusters is the rate-limiting step in the folding of an alanine-based peptide. Biopolymers 2003;68:63–75.
11. Jang S, Shin S, Pak Y. Molecular dynamics study of peptides in implicit water: ab initio folding of beta-hairpin,beta-sheet, and beta beta alpha- motif. J Am Chem Soc 2002;124:4976–4977.
12. Simmerling C, Strockbine B, Roitberg AE. All-atom structure prediction and folding simulations of a stable protein. J Am Chem Soc 2002;124:11258–11259.
13. Snow CD, Nguyen N, Pande VS, Gruebele M. Absolute comparison of simulated and experimental protein-folding dynamics. Nature 2002;420:102–106.
14. Tanizaki S, Feig M. A generalized Born formalism for heterogeneous dielectric environments: application to the implicit modeling of biological membranes. J Chem Phys 2005;122:124706.
15. Spassov VZ, Yan L, Szalma S. Introducing an implicit membrane in generalized Born/solvent accessibility continuum solvent models. J Phys Chem B 2002;106:8726–8738.
16. Im W, Feig M, Brooks CL III. An implicit membrane generalized born theory for the study of structure, stability, and interactions of membrane proteins. Biophys J 2003;85:2900–2918.
17. Im W, Brooks CL III. De novo folding of membrane proteins: an exploration of the structure and NMR properties of the fd coat protein. J Mol Biol 2004;337:513–519.
18. Im W, Chen JH, Brooks CL. Peptide and protein folding and conformational equilibria: theoretical treatment of electrostatics and hydrogen bonding with implicit solvent models. In: Baldwin RL, Baker D, editors. Peptide solvation and H-bonds, Vol 72: Advances in protein chemistry. San Diego: Elsevier Academic; 2006. p 173.
19. Tanizaki S, Feig M, Molecular dynamics simulations of large integral membrane proteins with an implicit membrane model. J Phys Chem B 2006;110:548–556.
20. Bu L, Im W, Brooks CL, III. Membrane assembly of simple helix homo-oligomers studied via molecular dynamics simulations. Biophys J 2007;92:854–863.
21. Im W, Brooks CL. Interfacial folding and membrane insertion of designed peptides studied by molecular dynamics simulations, Proceedings of the National Academy of Sciences of the United States of America. 2005;102:6771–6776.
22. Lee J, Im W. Implementation and application of helix-helix distance and crossing angle restraint potentials. J Comput Chem 2007;28: 669–680.
23. Zhou RH, Berne BJ. Can a continuum solvent model reproduce the free energy landscape of a beta-hairpin folding in water? Proc Natl Acad Sci USA 2002;99:12777–12782.
24. Hessa T, Kim H, Bihlmaier K, Lundin C, Boekel J, Andersson H, Nilsson I, White SH, von Heijne G. Recognition of transmembrane helices by the endoplasmic reticulum translocon. Nature 2005;433: 377–381.
25. Hessa T, White SH, von Heijne G. Membrane insertion of a potassium-channel voltage sensor. Science 2005;307:1427.
26. Totrov M. Accurate and efficient generalized born model based on solvent accessibility: derivation and application for LogP octanol/water prediction and flexible peptide docking. J Comput Chem 2004;25:609–619.
27. Okur A, Strockbine B, Hornak V, Simmerling C. Using PC clusters to evaluate the transferability of molecular mechanics force fields for proteins. J Comput Chem 2003;24:21–31.
28. Deechongkit S, Dawson PE, Kelly JW. Toward assessing the position-dependent contributions of backbone hydrogen bonding to beta-sheet folding thermodynamics employing amide-to-ester perturbations. J Am Chem Soc 2004;126:16762–16771.
29. Qiu D, Shenkin PS, Hollinger FP, Still WC. The GB/SA continuum model for solvation. A fast analytical method for the calculation of approximate Born radii. J Phys Chem A 1997;101:3005–3014.
30. Jorgensen WL, Ulmschneider JP, Tirado-Rives J. Free energies of hydration from a generalized Born model and an ALL-atom force field. J Phys Chem B 2004;108:16264–16270.
31. Parsegian A. Energy of an ion crossing a low dielectric membrane: solutions to four relevant electrostatic problems. Nature 1969;221: 844–846.
32. Schaefer M, Bartels C, Karplus M. Solution conformations and thermodynamics of structured peptides: molecular dynamics simulation with an implicit solvation model. J Mol Biol 1998;284:835–848.
33. Radzicka A, Wolfenden R. Comparing the polarities of the amino-acids—side-chain distribution coefficients between the vapor-phase, cyclohexane, 1-octanol, and neutral aqueous-solution. Biochemistry 1988;27:1664–1670.
34. Ulmschneider JP, Jorgensen WL. Monte Carlo backbone sampling for polypeptides with variable bond angles and dihedral angles

using concerted rotations and a Gaussian bias. J Chem Phys 2003; 118:4261–4271.
35. Jorgensen WL, Maxwell DS, Tirado-Rives J. Development and testing of the OPLS all-atom force field on conformational energetics and properties of organic liquids. J Am Chem Soc 1996;118:11225–11236.
36. Ulmschneider JP, Jorgensen WL. Monte Carlo backbone sampling for nucleic acids using concerted rotations including variable bond angles. J Phys Chem B 2004;108:16883–16892.
37. Ulmschneider JP, Ulmschneider MB, Di Nola A. Monte Carlo vs. molecular dynamics for all-atom polypeptide folding simulations. J Phys Chem B 2006;110:16733–16742.
38. Wang JF, Kim S, Kovacs F, Cross TA. Structure of the transmembrane region of the M2 protein H+ channel. Protein Sci 2001;10: 2241–2250.
39. Mascioni A, Karim C, Barany G, Thomas DD, Veglia G. Structure and orientation of sarcolipin in lipid environments. Biochemistry 2002;41:475–482.
40. Buffy JJ, Traaseth NJ, Mascioni A, Gor'kov PL, Chekmenev EY, Brey WW, Veglia G. Two-dimensional solid-state NMR reveals two topologies of sarcolipin in oriented lipid bilayers. Biochemistry 2006;45:10939–10946.
41. Buffy JJ, Buck-Koehntop BA, Porcelli F, Traasethl NJ, Thomas DD, Veglia G. Defining the intramembrane binding mechanism of sarcolipin to calcium ATPase using solution NMR spectroscopy. J Mol Biol 2006;358:420–429.
42. Sugita Y, Okamoto Y. Replica-exchange molecular dynamics method for protein folding. Chem Phys Lett 1999;314:141–151.
43. Earl DJ, Deem MW. Parallel tempering: theory, applications, and new perspectives. Phys Chem Chem Phys 2005;7:3910–3916.
44. Chakrabartty A, Kortemme T, Baldwin RL. Helix propensities of the amino-acids measured in alanine-based peptides without helix-stabilizing side-chain interactions. Protein Sci 1994;3:843–852.
45. Shalongo W, Dugad L, Stellwagen E. Distribution of helicity within the model peptide acetyl(Aaqaa)(3)amide 1994;116:8288–8293.
46. Ferrara P, Apostolakis J, Caflisch A. Thermodynamics and kinetics of folding of two model peptides investigated by molecular dynamics simulations. J Phys Chem B 2000;104:5000–5010.
47. Chen JH, Im WP, Brooks CL. Balancing solvation and intramolecular interactions: toward a consistent generalized born force field. J Am Chem Soc 2006;128:3728–3736.
48. Sung SS, Wu XW. Molecular dynamics simulations of synthetic peptide folding. Proteins 1996;25:202–214.
49. Shirley WA, Brooks CL. Curious structure in "canonical" alanine based peptides. Proteins 1997;28:59–71.
50. Wu XW, Sung SS. Simulation of peptide folding with explicit water—a mean solvation method. Proteins 1999;34:295–302.
51. Wu XW, Wang SM. Helix folding of an alanine-based peptide in explicit water. J Phys Chem B 2001;105:2227–2235.
52. Hassan SA, Mehler EL. A general screened Coulomb potential based implicit solvent model: calculation of secondary structure of small peptides. Int J Quantum Chem 2001;83:193–202.
53. Shental-Bechor DS, Kirca S, Ben-Tal N, Haliloglu T. Monte Carlo studies of folding, dynamics, and stability in alpha-helices. Biophys J 2005;88:2391–2402.
54. Cristian L, Lear JD, Degrado WF. Determination of membrane protein stability via thermodynamic coupling of folding to thiol-disulfide interchange. Protein Sci 2003;12:1732–1740.
55. Howard KP, Lear JD, DeGrado WF. Sequence determinants of the energetics of folding of a transmembrane four-helix-bundle protein. Proc Natl Acad Sci USA 2002;99:8568–8572.
56. Torres J, Kukol A, Arkin IT. Use of a single glycine residue to determine the tilt and orientation of a transmembrane helix. A new structural label for infrared spectroscopy. Biophys J 2000;79:3139–3143.
57. Salom D, Hill BR, Lear JD, DeGrado WF. pH-dependent tetramerization and amantadine binding of the transmembrane helix of M2 from the influenza A virus. Biochemistry 2000;39:14160–14170.
58. Pinto LH, Dieckmann GR, Gandhi CS, Papworth CG, Braman J, Shaughnessy MA, Lear JD, Lamb RA, DeGrado WF. A functionally defined model for the M-2 proton channel of influenza A virus suggests a mechanism for its ion selectivity. Proc Natl Acad Sci USA 1997;94:11301–11306.
59. Nishimura K, Kim SG, Zhang L, Cross TA. The closed state of a H+ channel helical bundle combining precise orientational and distance restraints from solid state NMR-1. Biochemistry 2002;41: 13170–13177.
60. Kovacs FA, Denny JK, Song Z, Quine JR, Cross TA. Helix tilt of the M2 transmembrane peptide from influenza A virus: an intrinsic property. J Mol Biol 2000;295:117–125.
61. Forrest LR, DeGrado WF, Dieckmann GR, Sansom MSP. Two models of the influenza A M2 channel domain: verification by comparison. Fold Des 1998;3:443–448.
62. Forrest LR, Kukol A, Arkin IT, Tieleman DP, Sansom MSP. Exploring models of the influenza A M2 channel: MD simulations in a phospholipid bilayer. Biophys J 2000;78:55–69.
63. Sansom MS, Kerr ID, Smith GR, Son HS. The influenza A virus M2 channel: a molecular modeling and simulation study. Virology 1997;233:163–173.
64. Duong-Ly KC, Nanda V, Degrad WF, Howard KP. The conformation of the pore region of the M2 proton channel depends on lipid bilayer environment. Protein Sci 2005;14:856–861.
65. Wu Y, Voth GA. A computational study of the closed and open states of the influenza a M2 proton channel. Biophys J 2005;89: 2402–2411.
66. White SH, Wimley WC. Membrane protein folding and stability: physical principles. Annu Rev Biophys Biomol Struct 1999;28:319–365.
67. de Planque MRR, Killian JA. Protein-lipid interactions studied with designed transmembrane peptides: role of hydrophobic matching and interfacial anchoring (Review). Mol Membr Biol 2003;20:271–284.
68. Toyoshima C, Nakasako M, Nomura H, Ogawa H. Crystal structure of the calcium pump of sarcoplasmic reticulum at 2.6 angstrom resolution. Nature 2000;405:647–655.

 DOI 10.1002/prot